ISSN 2706-655X Vol.5, Issue 2: 11-16, DOI: 10.25236/IJFET.2023.050203

# Simulation Design and Characteristic Research of Electromagnetic Metasurface Absorber

**Lingbo Zhao[1], Zhijiang Zhong[2,*]**

[1]*College of Science, Donghua University, Shanghai, China*
[2]*School of Information Science and Technology, Southwest Jiaotong University, Chengdu, China*
**Corresponding author: dhuzlb@163.com*

***Abstract:*** *Electromagnetic metasurface technology is one of the most promising technologies for electromagnetic energy regulation. It is formed by an artificial periodic structure of discrete subwavelengths at the interface, allowing wavefront control and polarization control at the subwavelength scale, exhibiting a variety of special electromagnetic response capabilities, including abnormal beam bending, polarization transformation, electromagnetic wave absorption, etc. We propose a wide-angle, polarization-insensitive infrared perfect metasurface absorber made of an opaque gold ground layer, a dielectric spacer layer, and a hole-shaped gold patch on the spacer layer. The absorption spectrum of the metasurface absorber is simulated by the finite element method, and the results show that the absorber produces an absorption peak with a maximum absorption rate of 99.91% and a half-height and full width of 0.52um in the visible light band.*

***Keywords:*** *metasurface; electromagnetic perfect absorption; finite element method; absorption spectrum*

## 1. Introduction

Metamaterial is a special man-made material that can perform many functions not found in natural materials [1,2]. From the perspective of technology, the three-dimensional structure construction of metamaterials will bring great difficulties in manufacturing and implementation. Moreover, metamaterials have the disadvantages of high loss and strong dispersion [3,4]，to a large extent, its practical application is limited. To overcome these shortcomings of metamaterials, metasurface structures were proposed. [5] Metasurfaces are two-dimensional metamaterials with sub-wavelength thicknesses consisting of periodic microstructures of metal or dielectric materials, and have been proposed for various applications due to their ultra-thin thickness, extremely low losses, and ease of process manufacturing. In addition, metasurfaces demonstrate the ability to manipulate electromagnetic (EM) waves in microwaves and optical frequencies. For example, optical holography [6], planar lenses[7], perfect absorbers [8], invisible materials [9], polarization converters [10], etc. Among them, the study of electromagnetic wave absorption has always been a research hotspot in the field of electromagnetism, which is crucial in both engineering applications and national defence and military affairs.

Landy et al. [11] first proposed a perfect electromagnetic metasurface absorber in 2008. They designed a three-layer structure, the top layer is a metal open resonant ring structure, providing an electrical resonance response, and the magnetic resonance response is obtained by the magnetic field in the intermediate dielectric layer by excitation of the central metal bar of the top open resonant ring with the reverse parallel current in the underlying metal wire. By manipulating the geometric parameters of the structure, an absorption rate of up to 99% was obtained at 11.65 GHz. Moreover, the perfect electromagnetic metasurface absorber is less than 1/30th the thickness of a wavelength, a pioneering work that soon inspired a series of follow-up studies that operate in frequency bands ranging from microwave to visible light. Among many electromagnetic wave absorption, electromagnetic metasurface absorbers can be widely used in electromagnetic stealth, electromagnetic shielding, thermal imaging, thermal emitters, sensors and other fields because of their thin thickness, small size, simple structure and high absorption rate.

The mid-infrared absorber strategy also includes composite grating superabsorbers [12], photonic crystal superabsorbers [13], and broadband nanoresonator absorbers [14]. Liu et al. [15] designed a single-band infrared absorber using cross-patterned metamaterials. Ye et al. [16] further investigated

ISSN 2706-655X Vol.5, Issue 2: 11-16, DOI: 10.25236/IJFET.2023.050203

the omnidirectional and polarization insensitive characteristics of the crossover structure. Due to the limitations of single-band IR absorbers in applications such as spectroscopy and imaging [17], dual- or multi-band IR absorbers and emitters are more desirable. Liu et al. [18] further investigated the dual-band absorber by transversely assembling one subunit into the original cross-patterned unit cell. Chen et al. [19] studied the dual-band perfect absorber by breaking the symmetry of the crossover structure, but the asymmetric structure is always polarization sensitive to the incident wave. Further dual-band perfect absorbers were designed, using elliptical nanodisks in the near-infrared band [20] and electric field-coupled resonators in the far-infrared band [21].

In this paper, a perfect electromagnetic metasurface absorber that is insensitive to polarization and angle of incidence is proposed, including a hole-shaped gold patch and gold ground plane and a SiC dielectric spacer layer. Perfect absorption of up to 99.91% was obtained at an angle of incidence θ = 45°. In addition, the reasons for the perfect absorption are theoretically analyzed.

## 2. Structural design

Figure 1 shows a schematic diagram of the structural blocks of the proposed perfect electromagnetic metasurface absorber. The structure consists of gold as the top layer, SiC as the intermediate medium layer and gold substrate. Among them, the dielectric function of gold is selected as the Drude model, ie

$$\varepsilon_m(\omega) = 1 - \omega_p^2 / \omega\left(\omega + i\omega_c\right) \tag{1}$$

Among them, plasma frequency $\omega_c = 1.2\times10^{16} rad/s$ and collision frequency $\omega_c = 10.5\times10^{13} rad/s$ [22]. The SiC layer was selected as the dielectric spacer layer, with a dielectric constant of 10.8 and a loss tangent of 0.003. The thickness of the SiC layer and the gold layer are td = 0.27 um and tm = 0.1 um, respectively. The lattice period of the structure in the X and Y directions is Λ = 2.6um. The middle hole-shaped structure has a width of L and a hole radius of r. The transport and reflection coefficients of the proposed structure are calculated by the finite element method solver. As shown in Figure 1(c), if there is a transverse magnetic (TM) wave incident into the structure on the x-z incident plane (where azimuth φ=0°, that is, the projection of the incident ray in the x-y plane and the x-direction is 0°), then there will be an electric field in the x-z plane and a magnetic field in the y direction. In the model construction of the finite element method solver, periodic boundary conditions need to be used in the x and y directions to form a periodic surface structure of the metasurface.

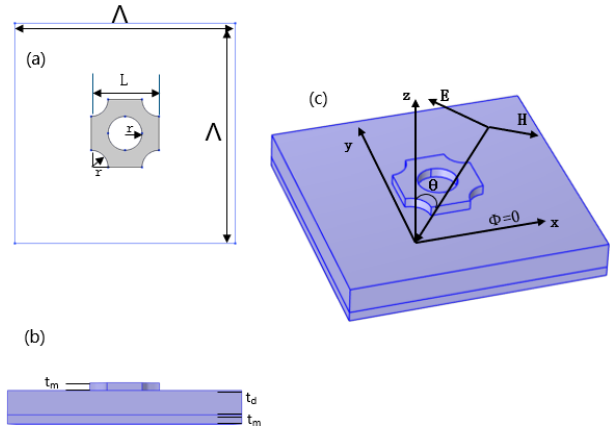


*Figure 1 (a) Top view and (b) side view of a unit cell of hole shaped metasurface absorber, (c) TE configuration impinging on the structure in $x-z$ incident plane (where the azimuthal angle φ = 0°) with an incident angle of $\theta$ to $z$ –direction.*

## 3. Theoretical analysis and discussion

The key to achieving a perfectly absorbing metasurface is to match the impedance of the metasurface to the air. Impedance matching allows the incident wave to enter the metasurface without

ISSN 2706-655X Vol.5, Issue 2: 11-16, DOI: 10.25236/IJFET.2023.050203

reflection and dissipate the energy of the incident electromagnetic wave through ohmic losses in the metasurface. The metasurface behaves as a complex equivalent electromagnetic parameter that satisfies the following impedance matching relationship:

$$Z_{eff} = \sqrt{\frac{\mu_0 \mu_{eff}}{\varepsilon_0 \varepsilon_{eff}}} = Z_0 \tag{2}$$

Among them, $Z_{eff}$ and $Z_0$ are equivalent wave impedances of metasurfaces and wave impedances in free space, respectively, and $\mu_0$ and $\varepsilon_0$ are magnetic permeability and vacuum permittivity, respectively. According to Equation (2), impedance matching requires $\varepsilon_{eff} = \mu_{eff}$.

According to coupling mode theory, the metasurface of such a three-layer structure in Figure (1) can be equivalent as a single-channel resonator coupled to an external light wave, and its reflection coefficient is[23]:

$$r = -1 + \frac{2/\tau_r}{-i(\omega - \omega_0) + 1/\tau_a + 1/\tau_r} \tag{3}$$

where ω0 is the resonance angle frequency of the metasurface, ω is the incident light angle frequency,and τa and τr are the resonance state lifetimes caused by ohmic loss and radiation loss, respectively. $Q_a = \frac{\omega_0 \tau_a}{2}$ and $Q_r = \frac{\omega_0 \tau_r}{2}$ describe the absorption and radiation quality factors of the system, respectively, and they depend on the geometric parameters of the metasurface element. From Equation (3), when $\omega = \omega_0$, the reflectance coefficient is determined entirely by $Q_a$ and $Q_r$. By adjusting the parameters of the top metal structure and the thickness of the intermediate dielectric layer, $Q_a = Q_r$ can be made. In this case, $r = 0$.

Since the metal substrate eliminates the transmission channel,absorption is determined by $A = 1 - |S_{11}|^2$, where $|S_{11}|$ indicates the reflectance coefficient. For TE and TM configurations, simulated absorption spectra for hole-shaped structures with different angles of incidence over the entire operating range ( $5\mu m - 8\mu m$ ) are shown in Figures 2(a) and 2(b).

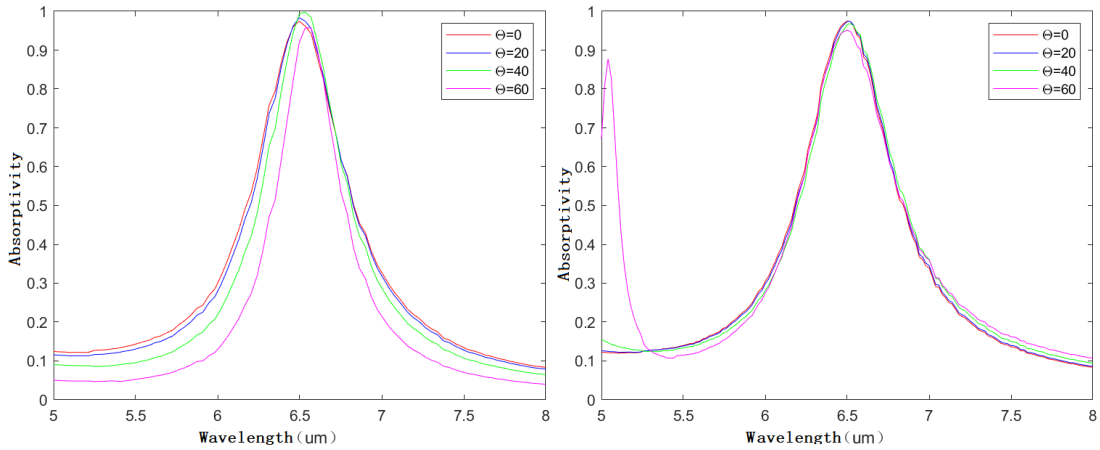


*Figure 2 Absorption spectra of hole shaped metasurface absorber with an incidence angle of* $45^\circ$ *for TE configuration and TM configuration, where the azimuthal angle* $\varphi = 0^\circ$ *and the length* $l$ *and radius* $r$ *are respectively set as* $0.8\mu m$ *and* $0.2\mu m$.

The hole-shaped metasurface at the $\varphi = 0^\circ$ incidence surface has high absorption (greater than 90%) and wide angle of incidence absorption stability at TE incidence and TM incidence and is insensitive to polarization. However, the absorption stability in TE mode is not as good as in TM mode

ISSN 2706-655X Vol.5, Issue 2: 11-16, DOI: 10.25236/IJFET.2023.050203

because the magnetic field strength in the x-y plane decreases with the increase of the angle of incidence $\theta$, so the poles that contribute to strong absorption cannot be effectively excited. In addition, the oscillation direction of the magnetic poles in the structure is related to the azimuth $\varphi$, which has an effect on the absorption stability.

Figures 3 and 4 show the distribution of the Z component of the electric field on the hole-shaped patch and the bottom metal layer at TE and TM incidence at resonant wavelengths λ = 6.53 μm, respectively. As can be seen from Figure 3(a), the electric field is mainly distributed in the tail region of the hole-shaped patch, while the top electric field is weak. In addition, at the same resonant wavelength, the electric field distribution across the bottom metal layer is shown in Figure 3(b), which is the opposite sign compared to the electric field distribution on the hole-shaped patch, indicating that an induced current loop is formed between the SiC dielectric spacer layers. This characteristic of the electric field distribution indicates that the poles are excited in each periodic hole-shaped structural gold patch, resulting in magnetic resonance, based on the analysis of the effective medium theory, the absorption is attributed to proximal electric and magnetic dipole resonances[24].

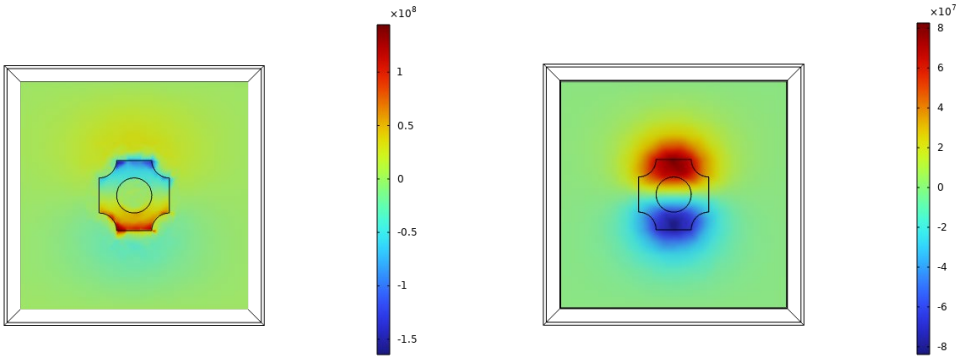


*Figure 3 The z component of electric field distribution at resonant wavelength λ = 6.53 μm on (a) hole-shaped patches and (b) bottom metal layer in TE configuration under the incident angle of θ = 45° and φ = 0°.*

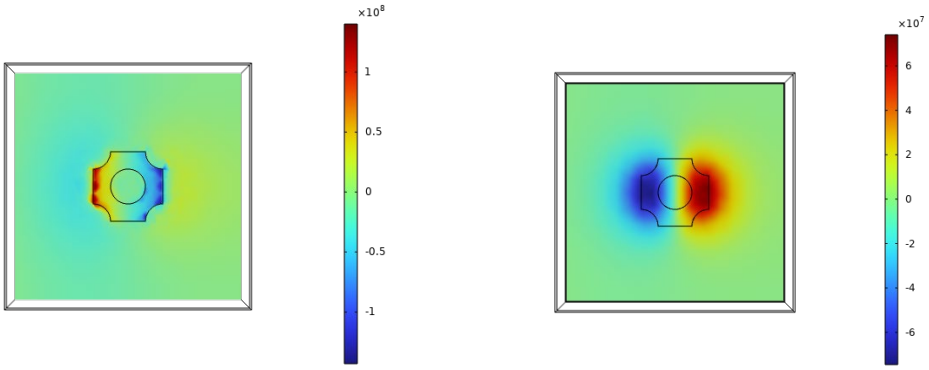


*Figure 4 The z component of electric field distribution at resonant wavelength λ = 6.53 μm on (a) hole-shaped patches and (b) bottom metal layer in TM configuration under the incident angle of θ = 45° and φ = 0°.*

For the stability of absorption when the incidence angle θ changes from 0° to 80°, Figure 5(a) shows the TE polarization incidence and Figure 5(b) shows the TM polarization incidence condition, where azimuth φ=0°. Under TE polarization incidence conditions, high absorption of up to 99% is achieved when θ varies from 0° to 60°, where the highest absorption is obtained at θ=45°. With the angle of incidence greater than 60°, the intensity of the two absorption peaks decreases rapidly. This is because magnetic polarizers require a magnetic field component in the X-Y plane to excit. For TE incidence, the magnetic field in the x-y plane is Hx-y = Hcosθ, where H is the strength of the incident magnetic field. Due to the rapid decrease in intensity at θ>60°, the magnetic resonance becomes weaker. In the TM configuration where θ varies from 0° to 80°, the strength of the absorption peak is still above 99%, due to the stable component of the incident magnetic field in the direction of the

ISSN 2706-655X Vol.5, Issue 2: 11-16, DOI: 10.25236/IJFET.2023.050203

oscillation of the poles. At the same time, the two absorption peaks undergo a slight blue shift with the change of θ, which is mainly due to the separation oscillation effect in each cell [25].

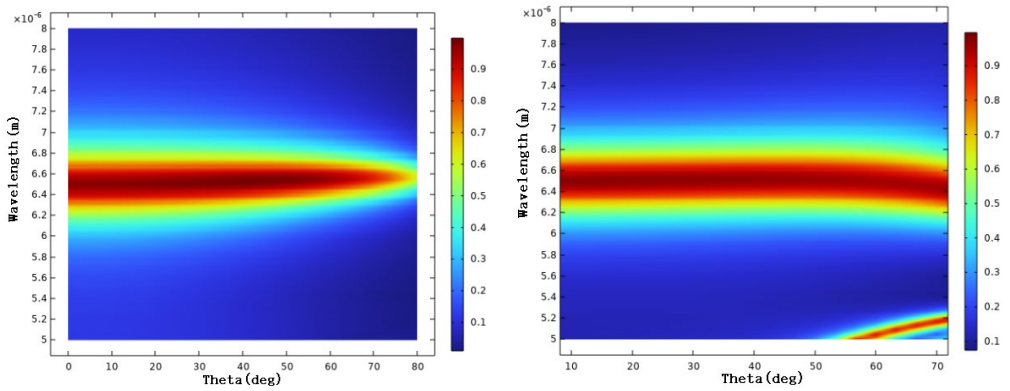


*Figure 5 Absorption spectra as a function of incidentangle θ at φ = 0° (a) for TE configuration and (b) for TM configuration, and the intensity of absorption is given by the colormap.*

## 4. Conclusion

Metamaterial absorbing devices have become a research hotspot in the field of micro-nano optics in recent years, usually classified according to the absorption bandwidth, which can be divided into two categories: narrowband absorbers and broadband absorbers. Narrowband absorbers are commonly used for optical sensing, and broadband absorbers are widely used in solar cells, photoelectric detection, imaging and other fields. At present, for micro-nano structures, many narrowband and broadband absorbing devices with different surface types and absorption mechanisms have been designed, and the research band has also expanded from the initial microwave and terahertz bands to infrared, visible and ultraviolet bands. Micro-nano absorbing devices usually only require sub-wavelength physical thickness, but can achieve good enhanced absorption performance, which is conducive to on-chip integration and packaging of optical components, so it has great advantages in applications. We have numerically demonstrated the absorption characteristics of electromagnetic metasurface perfect absorbers in the infrared region. The absorber includes a hole-shaped gold patch and gold ground plane and a SiC dielectric spacer layer. A perfect absorption peak is obtained at an angle of incidence θ = 45°. Absorption spectra with bearing are also studied.According to the distribution of the z-component of the electric field distribution within the absorber, we get that the perfect absorption is caused by the excitation of magnetic polarizers at the resonant wavelength. In addition, electromagnetic metasurface perfect absorbers also exhibit good absorption stability in the wide azimuth and incidence range of TE and TM incidence. This wide-angle, polarization-insensitive perfect infrared absorber offers potential applications for heat detectors and infrared imaging.

## References

*[1] Badri, S. H., Gilarlue, M. M., SaeidNahaei, S., & Kim, J. S. (2022). Narrowband-to-broadband switchable and polarization-insensitive terahertz metasurface absorber enabled by phase-change material. Journal of Optics, 24(2), 025101.*

*[2] Schurig, D., Mock, J. J., Justice, 1. B., Cummer, S. A., Pendry, J. B., Starr, A. F., & Smith, D. R. (2006). Metamaterial electromagnetic cloak at microwave frequencies. Science, 314(5801), 977-980.*

*[3] Wang, H. L., Ma, H. F., Chen, M., Sun, S., & Cui, T. J. (2021). A Reconfigurable Multifunctional Metasurface for Full-Space Control of Electromagnetic Waves. Advanced Functional Materials, 31(25), 2100275.*

*[4] Bukhari, S. S., Vardaxoglou, J., & Whittow, W. (2019). A metasurfaces review: Definitions and applications. Applied Sciences, 9(13), 2727.*

*[5] Chen, H. T., Taylor, A. J., & Yu, N. (2016). A review of metasurfaces: physics and applications. Reports on progress in physics, 79(7), 076401.*

*[6] Khorasaninejad, M., Chen, W. T., Devlin, R. C., Oh, J., Zhu, A. Y., & Capasso, F. (2016). Metalenses at visible wavelengths: Diffraction-limited focusing and subwavelength resolution imaging. Science, 352(6290), 1190-1194.*

*[7] Aieta, F., Genevet, P., Kats, M. A., Yu, N., Blanchard, R., Gaburro, Z., & Capasso, F. (2012).*

ISSN 2706-655X Vol.5, Issue 2: 11-16, DOI: 10.25236/IJFET.2023.050203

*Aberration-free ultrathin flat lenses and axicons at telecom wavelengths based on plasmonic metasurfaces. Nano letters, 12(9), 4932-4936.*
*[8] Nguyen, T. Q. M., Nguyen, T. K. T., Le, D. T., Truong, C. L., Vu, D. L., & Nguyen, T. Q. H. (2021). Numerical study of an ultra-broadband and wide-angle insensitive perfect metamaterial absorber in the UV–NIR region. Plasmonics, 16(5), 1583-1592.*
*[9] Shao, K., Shu, L., Wang, Q., Liu, M., Tian, Q., & Hu, W. (2015). Quantum Stealth Technology. J. Org. Chem. Res, 3, 66-76.*
*[10] Nguyen, T. Q. H., Nguyen, T. K. T., Nguyen, T. Q. M., Cao, T. N., Phan, H. L., Luong, N. M., ... & Vu, D. L. (2021). Simple design of a wideband and wide-angle reflective linear polarization converter based on crescent-shaped metamaterial for Ku-band applications. Optics Communications, 486, 126773.*
*[11] Yeo, W. G., Nahar, N. K., & Sertel, K. (2013). Far-IR multiband dual-polarization perfect absorber for wide incident angles. Microwave and Optical Technology Letters, 55(3), 632-636.*
*[12] Liu, X., Starr, T., Starr, A. F., & Padilla, W. J. (2010). Infrared spatial and frequency selective metamaterial with near-unity absorbance. Physical review letters, 104(20), 207403.*
*[13] Ye, Y. Q., Jin, Y., & He, S. (2010). Omnidirectional, polarization-insensitive and broadband thin absorber in the terahertz regime. JOSA B, 27(3), 498-504.*
*[14] Christensen, P. R., Jakosky, B. M., Kieffer, H. H., Malin, M. C., McSween, H. Y., Nealson, K., ... & Ravine, M. (2004). The thermal emission imaging system (THEMIS) for the Mars 2001 Odyssey Mission. Space Science Reviews, 110, 85-130.*
*[15] Liu, X., Tyler, T., Starr, T., Starr, A. F., Jokerst, N. M., & Padilla, W. J. (2011). Taming the blackbody with infrared metamaterials as selective thermal emitters. Physical review letters, 107(4), 045901.*
*[16] Chen, K., Adato, R., & Altug, H. (2012). Dual-band perfect absorber for multispectral plasmon-enhanced infrared spectroscopy. ACS nano, 6(9), 7998-8006.*
*[17] Zhang, B., Zhao, Y., Hao, Q., Kiraly, B., Khoo, I. C., Chen, S., & Huang, T. J. (2011). Polarization-independent dual-band infrared perfect absorber based on a metal-dielectric-metal elliptical nanodisk array. Optics express, 19(16), 15221-15228.*
*[18] Tao, H., Bingham, C. M., Pilon, D., Fan, K., Strikwerda, A. C., Shrekenhamer, D. & Averitt, R. D. (2010). A dual band terahertz metamaterial absorber. Journal of physics D: Applied physics, 43(22), 225102.*
*[19] Yeo, W. G., Nahar, N. K., & Sertel, K. (2013). Far-IR multiband dual-polarization perfect absorber for wide incident angles. Microwave and Optical Technology Letters, 55(3), 632-636.*
*[20] Qu, C., Ma, S., Hao, J., Qiu, M., Li, X., Xiao, S. & Zhou, L. (2015). Tailor the functionalities of metasurfaces based on a complete phase diagram. Physical review letters, 115(23), 235503.*
*[21] Ye, Y. Q., Jin, Y., & He, S. (2010). Omnidirectional, polarization-insensitive and broadband thin absorber in the terahertz regime. JOSA B, 27(3), 498-504.*
*[22] Mason, J. A., Smith, S., & Wasserman, D. J. A. P. L. (2011). Strong absorption and selective thermal emission from a midinfrared metamaterial. Applied Physics Letters, 98(24), 241105.*
*[23] Devarapu, G. C. R., & Foteinopoulou, S. (2012). Mid-IR near-perfect absorption with a SiC photonic crystal with angle-controlled polarization selectivity. Optics express, 20(12), 13040-13054.*
*[24] Dai, W., Yap, D., & Chen, G. (2012). Wideband enhancement of infrared absorption in a direct band-gap semiconductor by using nonabsorptive pyramids. Optics Express, 20(104), A519-A529.*
*[25] Huang, Y., Kaj, K., Chen, C., Yang, Z., Ul Haque, S. R., Zhang, Y. & Zhang, X. (2022). Broadband terahertz silicon membrane metasurface absorber. ACS Photonics, 9(4), 1150-1156.*